INTERNATIONAL JOURNAL OF CLIMATOLOGY
Int. J. Climatol. (2008)
Published online in Wiley InterScience
(www.interscience.wiley.com) DOI: 10.1002/joc.1683

RMetS
ROYAL METEOROLOGICAL SOCIETY

Interannual variability of atmospheric water balance over South Peninsular India and Sri Lanka during northeast monsoon season

Venkatraman Prasanna[a]* and Tetsuzo Yasunari[b]

[a] *Graduate School of Environmental Studies, Nagoya University, Nagoya, Aichi, 464-8601, Japan*
[b] *Hydrospheric Atmospheric Research Center, Nagoya University, Nagoya, Aichi, 464-8601, Japan*

ABSTRACT: In this study we have investigated atmospheric water balance over South Peninsular India and Sri Lanka during the months October to December (OND) using computed moisture convergence (C) and residual evaporation (E) from National Centers for Environmental Prediction/National Center for Atmospheric Research (NCEP/NCAR) reanalysis data and Global Precipitation and Climatology Project (GPCP) precipitation data. The interannual signatures of OND precipitation, moisture convergence and evaporation over the South Peninsular India and Sri Lanka have been captured. The spatial and temporal characteristics of the hydrological cycle and the contribution of evaporation (E) and convergence (C) to precipitation (P) are discussed in detail. Over the South Peninsular India and Sri Lanka, evaporation (E) dominates during the entire monsoon months (OND). However, the interannual variability of precipitation over the domain is not necessarily influenced by the same criteria which influences the mean seasonal precipitation. The moisture from the Indian Ocean (IO) sector also modulates the precipitation over this region on a year-to-year basis. It has been noted that the positive northeast monsoon rainfall (NEMR) is associated with El Nino coupled with IO dipole, but negative NEMR is weakly associated only with La Nina over South Peninsular India and Sri Lanka. There also exists a significant land-atmospheric interaction over the region in modulating the hydrological cycle on a year-to-year basis. Copyright © 2008 Royal Meteorological Society

KEY WORDS atmospheric water balance; interannual variability; Indian Ocean Dipole

Received 20 June 2007; Revised 27 September 2007; Accepted 23 December 2007

1. Introduction

Two vital monsoon systems prevail over the Indian subcontinent, namely, the summer monsoon [also known as southwest (SW) monsoon] and northeast (NE) monsoon (retreating monsoon). The SW monsoon has been studied widely compared to the NE monsoon. Monsoon is forced primarily due to the seasonal shifting of thermally produced planetary belts of pressure and winds under continental influences. The heating over oceans and extensive cooling over the continental areas facilitate the northeastward flow of winds over the Bay of Bengal (BOB) and thus, the moisture carried from the BOB creates a favourable condition for NE monsoon to develop over the South Peninsular India and Sri Lanka during October to December (OND). Post-monsoon season or simply the northeast monsoon rainfall (NEMR) season (OND) over South Peninsular India and Sri Lanka is the major rainfall season over this region (Dhar and Rakhecha, 1983), which helps agricultural production in this region (Kumar *et al*., 2007). NEMR received very less attention in terms of studies in interannual variability and its teleconnections (Singh and Sontakke, 1999; Kripalani and Kumar, 2004; Kumar *et al*., 2007) and over the Sri Lankan region Suppiah (1989, 1996, 1997).

While most parts of India receive nearly the entire portion of their annual rainfall from the southwest monsoon rainfall (SWMR), the Southeast Peninsular India falls under the rain shadow region during the summer season due to the presence of Western Ghats. This region therefore critically depends on the NEMR to supplement the inadequate precipitation during SWMR. Over the southeastern tip of the Indian Peninsula and neighbouring Sri Lanka, nearly 50% of the annual rainfall is received during the NEMR season. Hence, this study focusses on the NEMR variability.

The impact of El Nino/Southern Oscillation (ENSO) on the SWMR has been explored intensively (Rasmusson and Carpenter, 1983; Krishna Kumar *et al*., 1999; Ailikun and Yasunari, 2001; Chang *et al*., 2001; Kawamura *et al*., 2005). The El Nino years are generally associated with below-normal SWMR rainfall (Rasmusson and Carpenter, 1983; Yasunari, 1990) and above-normal NEMR rainfall (Suppiah, 1996, 1997). Recently Kumar *et al*. (2007) studied the ENSO–NEMR relationship prior to 1976 and the later periods and concluded that the ENSO–NEMR

* Correspondence to: Venkatraman Prasanna, Graduate School of Environmental Studies, Nagoya University, Nagoya, Aichi, 464-8601, Japan. E-mail: Prasanna@hyarc.nagoya-u.ac.jp

relationship has strengthened considerably in the recent decades.

Earlier studies have pointed out that a unique ocean-atmosphere mode exists in the Indian Ocean (IO), with anomalous warm sea surface temperatures (SSTs) over the western IO and anomalous cold SSTs in the eastern IO (Saji *et al*., 1999). This mode induces an unusual rainfall distribution in the surrounding areas, and is termed as the Indian Ocean dipole zonal mode (IODZM) (Hastenrath *et al*., 1993; Webster *et al*., 1999). This dipole mode modulates the Maha (September and October) rainfall over Sri Lanka (Zubair *et al*., 2003). Similar study on the NEMR over South Peninsular India (Kripalani and Kumar, 2004) had revealed that NEMR and the Indian Ocean dipole mode (IODM) are directly related, suggesting that the positive dipole phase enhances the NE monsoon activity and the negative dipole phase suppresses the NE monsoon activity. In viewing the previous studies on NEMR variability, only ocean-atmospheric coupling has been stressed in detail, whereas land-atmospheric interactions remain unknown; to study such a role the atmospheric water budget can provide some lead.

To understand mechanisms other than ocean -atmospheric interaction over this region, we have tried to exploit the advantages of atmospheric water balance method over South Peninsular India and Sri Lanka. A few earlier global water budget studies have shown the importance of water budget analysis (Oki *et al*., 1995; Trenberth and Guillemot, 1998; Trenberth, 1999). What can be gained by budget analysis? Through assessing convergence (C) and evaporation (E), we can understand the hydro meteorological aspect of precipitation (P) dynamics.

Objectively reanalysed, gridded four-dimensional datasets [National Centers for Environmental Prediction (NCEP), ERA-40 and JRA reanalysis] give us an opportunity to study water balance on global and regional scales. Though there are physical constraints in the closed water budget calculation and it may be imperfect to use observed precipitation (P) to close the reanalyses water budget, it provides an opportunity to obtain less observed variable evaporation (E) at each grid point on regional and global scale through the balance. Since the reanalysis simulated evaporation is heavily model-dependent and the simulated precipitation is constrained by the model's parameterization schemes, we have tried to utilize the advantage of monthly-observed precipitation (P) to find the evaporation as a residual.

The main motivation of the present study is to understand the nature of the large-scale water balance over South Peninsular India and Sri Lanka during NEMR season (OND) and to understand the mechanism behind year-to-year precipitation variability over this region. For this purpose, the space–time characteristics of monthly and NEMR (OND) interannual variations of precipitation (P), convergence of water vapour flux (C) and evaporation (E) during the period, starting from 1979 up to 2005 have been studied in detail. Particular attention is paid to understand where the precipitation (P) comes, i.e. from large-scale moisture convergence (C) due to atmospheric circulation and/or from evaporation (E) from the surface since both ocean-atmosphere interactions and land-atmosphere interactions are fundamental in understanding the variability of precipitation over this region. Another aspect is how P, C and E are modified on interannual time scale by the slowly varying boundary conditions and how they are related this is also explored in detail.

The structure of this article is as follows. Section 2 describes the datasets and the computational procedures used in this study. In Section 3, we discuss the seasonality of NE monsoon over South Peninsular India and Sri Lanka. In Section 4, we document the basic features of the monthly annual cycle of water balance components (E, P, C) and seasonal march of precipitation over the selected domain and Section 5 presents a discussion of the interannual variability of precipitation and atmospheric water balance components. Section 6 discusses NEMR index with various climatic indices. Section 7 discusses the teleconnection of NEMR with various climate anomalies and the aspect of large-scale anomalies of atmospheric water balance for excess and deficient monsoon phases, IODM phases and Nino-3.4 anomaly phases. In Section 8, the main conclusions and discussions are addressed.

2. Data and method of analysis

The period of analysis covers NEMR monsoon season of OND from 1979 up to 2005. The data products used are Global Precipitation and Climatology Project (GPCP) precipitation (Adler *et al*., 2003), Variability Analysis of Surface Climate Observations (VASClimO) land gridded precipitation dataset 1950–2000 (Beck *et al*., 2005). Daily upper level winds (u, v), specific humidity (q), geo-potential height (z), surface winds (u, v), surface level specific humidity (q) and sea level pressure (SLP) obtained from NCEP/National Center for Atmospheric Research (NCAR) reanalysis dataset (Kalnay *et al*., 1996) and the monthly SST for the period 1982–2005 from NOAA (NOAA optimum interpolated SST dataset) (Reynolds *et al*., 2002).

The atmospheric water budget equation can be written as (Peixoto and Oort, 1992),

$$<\partial W/\partial t> + <\nabla \cdot Q> = <E - P> \ldots\ldots\ldots \quad (1)$$

where (P) is precipitation, (E) is evaporation, and angled brackets denote the area average, precipitable water content (W), vertically integrated moisture flux vector (Q) and its divergence ($\nabla \cdot Q$).

On longer timescales like monthly or seasonal, under near equilibrium conditions, the time change of local available precipitable water content is negligible compared to the variations of large-scale convergence and evaporation (Oki *et al*., 1995; Trenberth, 1999). We approximate,

$$<\partial W/\partial t> \sim 0 \ldots\ldots\ldots\ldots\ldots\ldots \quad (2)$$

DOI: 10.1002/joc

Therefore we can approximately write,

$$P \sim C + E \ldots\ldots\ldots\ldots\ldots\ldots \quad (3)$$

Vertically integrated moisture flux vector (Q) is given by,

$$Q = 1/g_{P_t}\int^{Ps} q\mathbf{v}\mathrm{d}p \ldots\ldots\ldots\ldots\ldots \quad (4)$$

Where q is the specific humidity, $\mathbf{v}$ is the horizontal wind vector, Ps is the pressure at surface level and Pt is the pressure at the top of the atmosphere, g is gravitational acceleration. Vertical integration is performed from ground level (surface pressure level) to 300 hPa for the standard atmospheric pressure level (1000, 925, 850, 700, 600, 500, 400 and 300). We can neglect pressure levels above 300 hPa, as the specific humidity above this level is negligible. The moisture flux divergence which is the second term in the left-hand side of Equation (1), and the vertically integrated moisture fluxes are computed using the linear grids.

Water budget calculations and data analyses were performed for the 27-year period from January 1979 through December 2005 as the reliable precipitation data over both land and ocean are available from 1979. The total vertically integrated moisture convergence is computed for the above period from NCEP/NCAR reanalysis datasets. Evaporation is obtained as a residual from the precipitation and convergence. The mean monthly contribution of evaporation (E) or convergence (C) to precipitation (P) and the year-to-year change in evaporation (ΔE) or convergence (ΔC) to precipitation (ΔP) are used to understand the seasonal and interannual variability of NEMR (OND) season over South Peninsular India and Sri Lanka. Mathematically, divergence is a positive quantity and convergence is a negative quantity, but in this article, we have defined the computed convergence as positive values and divergence as negative values.

The study area over South Peninsular India and Sri Lanka is shown in Figure 1. During the summer monsoon season (JJA), the south peninsular region receives less rainfall compared to the rest of India due to the presence of Western Ghats (Figure 2(a)); the region is a rain shadow region for summer monsoon. Considerable amount of mean seasonal precipitation over this region is evident during NEMR season (OND) (Figure 2(b)). The annual contribution of OND precipitation exceeds 50% over Southeast Peninsular India and Sri Lanka (Figure 2(c)).

3. Seasonality over Peninsular India and Sri Lanka

To clearly distinguish the season over South Peninsular India and Sri Lanka, the monthly mean moisture flux vectors along 80E are shown in Figure 3(a) and the spatial mean pattern of moisture convergence and moisture flux vectors during OND season are shown in Figure 3(b). We can clearly notice the reversal of moisture transport vectors from southwesterlies to northeasterlies around 10N–12N during October (Figure 3(a)). Though the mean precipitation during September–November (SON) is higher than OND, the OND has been chosen as NEMR season by considering the wind field. The percentage contribution of annual precipitation exceeds 50% over south eastern coastal Peninsular India during OND and also the moisture transport vectors become completely northeasterlies during OND over this region.

4. Monthly annual cycle of atmospheric water budget over the selected domain

The monthly mean annual cycle of precipitation (P), evaporation (E) and convergence (C) over the selected domain containing both South Peninsular India and Sri Lanka are shown in Figure 4(a) and (b). Before explaining the relative contribution of (C) or (E) to precipitation (P) on monthly scale, let us briefly explain the seasonal march of precipitation over the domain.

4.1. Monthly evolution of precipitation over the PEN and SL domain

To examine the monthly precipitation evolution for (PEN and SL) the domain averaged monthly mean precipitation for the period 1979–2005 is plotted in Figure 4(a) from the GPCP dataset. The monthly annual rainfall pattern has a double peak, namely, first one at June and another one at October. The NEMR monsoon (OND) over this region exhibits a very short rainy season and relatively low magnitude of precipitation unlike the SW monsoon over the entire south Asian region. The precipitation amount gradually increases from March and attains a peak in the month of June and sustains the peak till July and slowly falls in the successive months, but does not fall completely; the second peak pattern appears in October. This

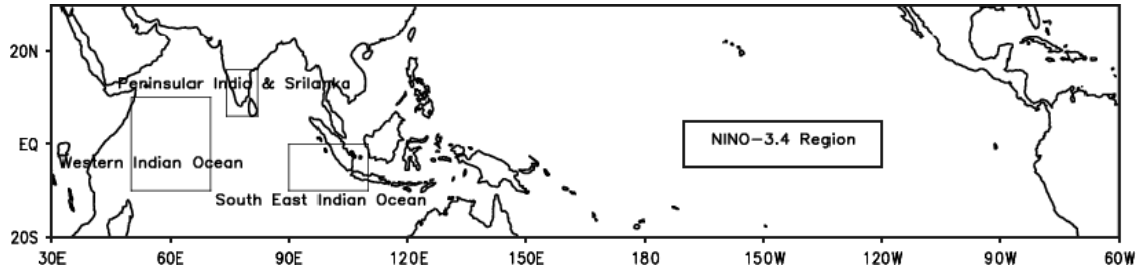

Figure 1. Maps showing selected domains for analysis in this study.

DOI: 10.1002/joc

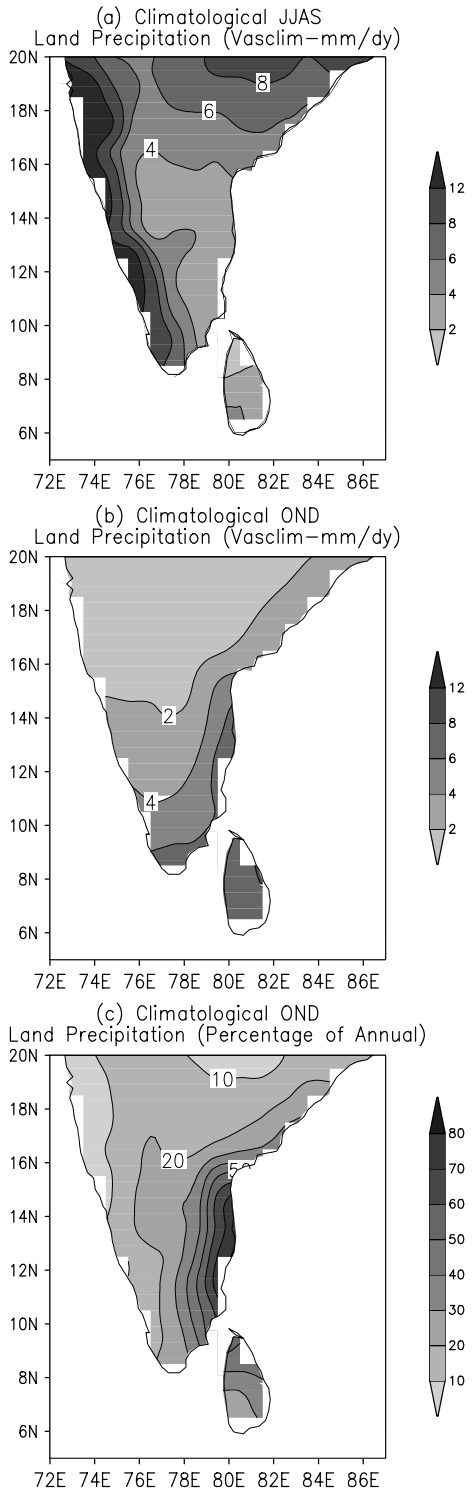

Figure 2. Climatological mean precipitation from VASClimO dataset for the period 1979–2000. (a) JJAS mean precipitation (mm/day) (b) Climatological mean OND precipitation (mm/day) (c) Percentage of OND precipitation contribution to annual mean precipitation.

is because of the precipitation from NE monsoon, mainly due to reversal of winds from southwesterly to northeasterly. The moisture carried from the BOB through northeasterly winds during OND brings precipitation over South Peninsular India and Sri Lanka. The NE monsoon precipitation (OND) is especially significant over the state of Tamil Nadu (Dhar and Rakhecha, 1983; Kumar *et al*., 2007). Nearly 50% of annual precipitation over this region is realized during the OND period.

4.2. Atmospheric water budget during NEMR season

Rainfall over the domain (Figure 4(b)) during the NEMR months (OND) are favoured by higher evaporation throughout the season shown in the box as (E). E is higher than P during pre-monsoon months and winter. Evaporation almost equals precipitation throughout the rainy season ($E \sim P$) (Figure 4(b)).

Over this region, convergence (C) becomes positive from June to November season. Convergence shows only one peak during July unlike precipitation during June and October for SW and NE monsoon months respectively. The double peak in the convergence is not very clear (Figure 4(b)), which may be due to the prevalence of weak convergence over Peninsular India. Strong convergence is seen only over Sri Lanka and the southeastern tip of Peninsular India implies that the mean evaporation during OND over South Peninsular India must be stronger than Sri Lanka.

Most of the earlier studies have shown that the ocean acts as a source of moisture during the NEMR monsoon months for this domain (Zubair *et al*., 2003; Kripalani and Kumar, 2004). Here, we have found that evaporation (E) is higher than convergence (C) in magnitude during OND and E contribution to precipitation (P) during the OND months is also significant. Thus, E contribution to precipitation P exceeds C contribution to P during OND months and the evaporation from the land surface also aids precipitation during the NEMR season.

5. Interannual variation of atmospheric water budget over Peninsular India and Sri Lanka

To study the precipitation variability on interannual time scale, the interannual variations of atmospheric water budget components are plotted for OND over the domain. The correlation coefficient (CC) between precipitation and moisture convergence are used to understand the relationship between P and C on the interannual time scale and similarly, for evaporation.

The contribution of evaporation to mean seasonal precipitation is high over South Peninsular India and the Sri Lankan region during NEMR monsoon period and also for interannual variability, the correlation between ΔP and ΔC is 0.73 (exceeds 95% significant level) and the correlation between ΔP and ΔE is 0.84 (exceeds 95% significant level) (Figure 4(c)); thus the contribution of evaporation during the monsoon months to the year-to-year variability of precipitation has been brought out through the atmospheric water budget clearly, i.e. $(\Delta E > \Delta C)$. The correlation between precipitation and the residual evaporation at 0.84 suggests that the land surface hydrological process are also important to understand the P variability on interannual timescales over this region.

One important point to be noted here is that the CC between ΔP and ΔC as well as ΔP and ΔE are highly

DOI: 10.1002/joc

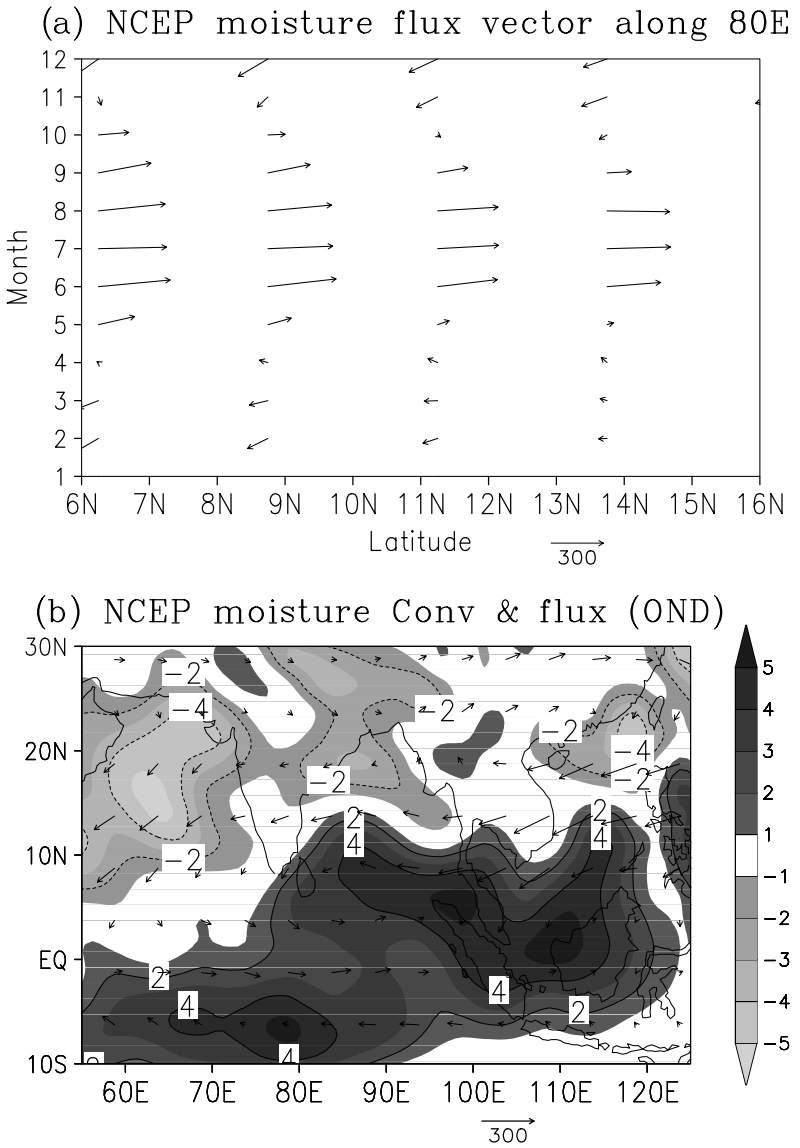

Figure 3. Maps of mean moisture convergence and moisture flux over the domain. (a) Monthly mean moisture flux for different latitudes along 80E (b) spatial pattern of moisture convergence and flux (OND). Positive values are darkly shaded and negative values are lightly shaded. (Units for convergence: mm/day, moisture flux: kg m^{-1} s^{-1}).

significant (significant above 95% level). Thus the P variability over this domain during NEMR season OND is not only dependent on the large-scale convergence ΔC, but also on ΔE. Strong land-atmospheric interactions do co-exist along with ocean-atmospheric interactions over this region during OND.

6. Averaged NEMR monsoon index *versus* IOD and NINO-3.4 indices

To identify the significant influence of various climate anomalies to NEMR variability (dominant climate anomalies like El Nino/La Nina and IOD anomalies), the NEMR precipitation index has been created using the observed GPCP precipitation over the selected domain and this index is used for discussing the strength of the monsoon over South Peninsular India and Sri Lanka during OND months as shown in Figure 5. Based on the available observed GPCP rainfall data, a time series of NEMR over South Peninsular India and Sri Lanka has been developed. Similarly, an index to quantify the IODM, exhibiting warm (cool) waters over the equatorial western (southeastern) IO and Nino-3.4 anomalies has been developed using (NOAA-IO) optimum interpolated SST data for the period (1982–2005).

The NEMR, IOD (Difference of SST between western Indian Ocean (WIO) (10S–10N, 55E–70E) and Southeast Indian Ocean (SEIO) (10S–0N, 90E–120E) and NINO-3.4 (5S–5N, 190E–240E) SST anomalies are standardized with their respective standard deviations (SDs) and plotted. We have considered OND season to represent the NEMR, whereas the IOD, El Nino and La Nina phases are represented by SON season, since the IOD peaks in the months of SON. Saji and Yamagata (2003) have shown that the largest combined contribution of ENSO and IOD to the zonal and meridional wind variability over the IO is during SON around

DOI: 10.1002/joc

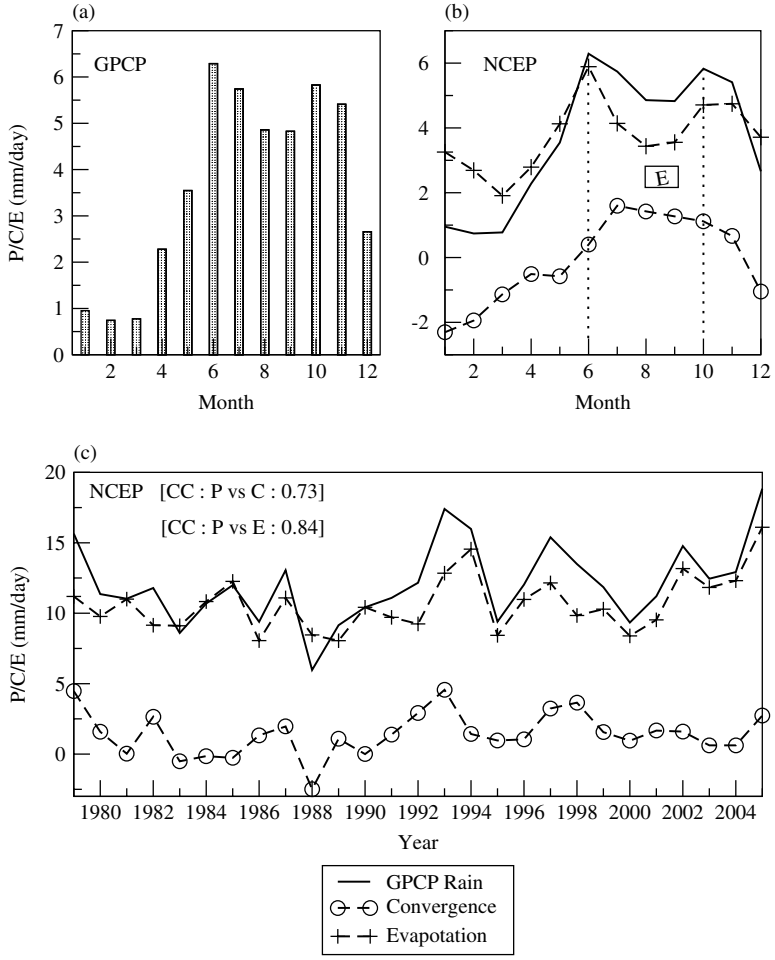

Figure 4. Observed monthly mean annual cycle of P, C and E over the selected domain (a) GPCP precipitation; (b) P, C, E (dominance of evaporation is shown as E in box) and (c) interannual variability of (OND) P, C and E over the selected domain (value of correlation coefficient between P, C and P, E are shown in graph).

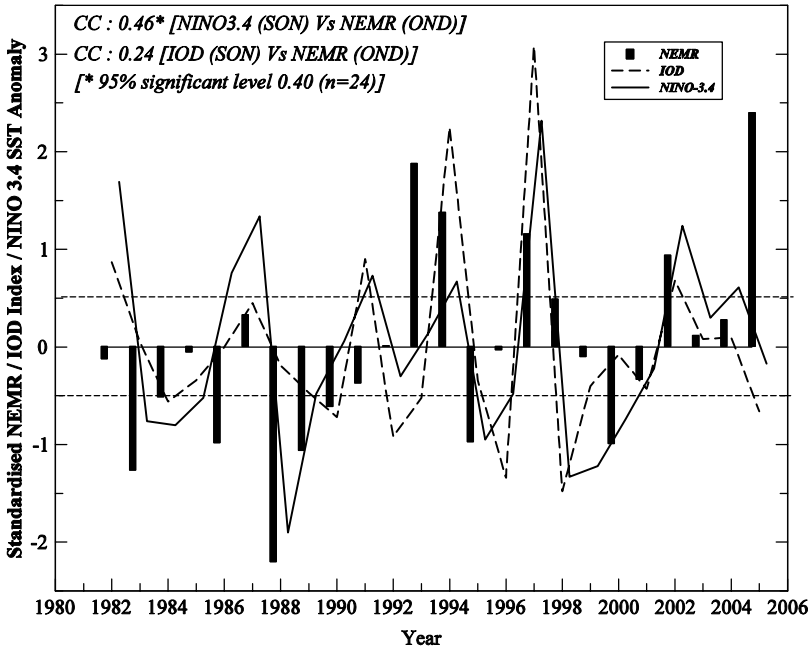

Figure 5. Standardised anomalies of NEMR over the selected domain (PEN & SL) during OND, IOD Indices during SON and NINO-3.4 SST anomalies during SON from 1982-2000. (Filled bars denote rainfall departures and dashed line denote IOD index and solid line denote Nino-3.4 SST anomalies. Horizontal dashed lines indicate departures of +/−0.5 standardised anomaly for NEMR, NINO 3.4 and +/−0.5 degree SST anomalies for IOD index).

DOI: 10.1002/joc

45% between 10S and 10N. The CC between NEMR and IOD is found to be less than the significant level (0.24), whereas the CC between NEMR and NINO-3.4 anomalies are significant (0.46*) at 95% significant level, which is also evident from the recent studies that the impact of ENSO on NEMR is strengthening in the recent decades (Kumar *et al*., 2007). The excess/deficient NEMR, IOD and NINO-3.4 positive/negative phase are obtained by applying a criterion that the standardized anomalies exceeds ±0.5 SD.

7. Teleconnections and large-scale anomalies of (*P*), (*C*) and (*E*) among anomalous NEMR, NINO-3.4 and Indian Ocean dipole mode years

In this section, we discuss the various teleconnections of NEMR and the differences in atmospheric circulation for anomalous NEMR monsoon years and IOD positive–negative phase years over the selected domain.

To show the teleconnection patterns of NEMR, the (NOAA-OI) optimum interpolated global SST (1982–2005) for OND is regressed with the selected domain's OND GPCP precipitation (Figure 6(b)). A significant positive correlation (significant at 95%) over the Nino-3.4 regions and over BOB near Myanmar coast and South China Sea, a less than significant negative correlation over the SEIO over the coast of Sumatra are noticed and no correlations are observed with IOD.

The regressed pattern of precipitation reveals a significant negative relationship with the Indo-China Peninsula precipitation during NEMR monsoon (OND) season (Figure 6(a)). Figure 6(c) shows that the convergence over IO is significantly associated with the domain precipitation, and the moisture flux vectors largely originate from the SEIO region. Figure 6(d) shows that evaporation also plays an active role in modulating the interannual variability of NEMR precipitation over the PEN & SL domain.

In Figures 7 and 8, anomalies of precipitation (*P*), large-scale convergence (*C*), moisture transport vectors and evaporation (*E*) are plotted for anomalous NEMR monsoon years, IOD positive–negative phase years and

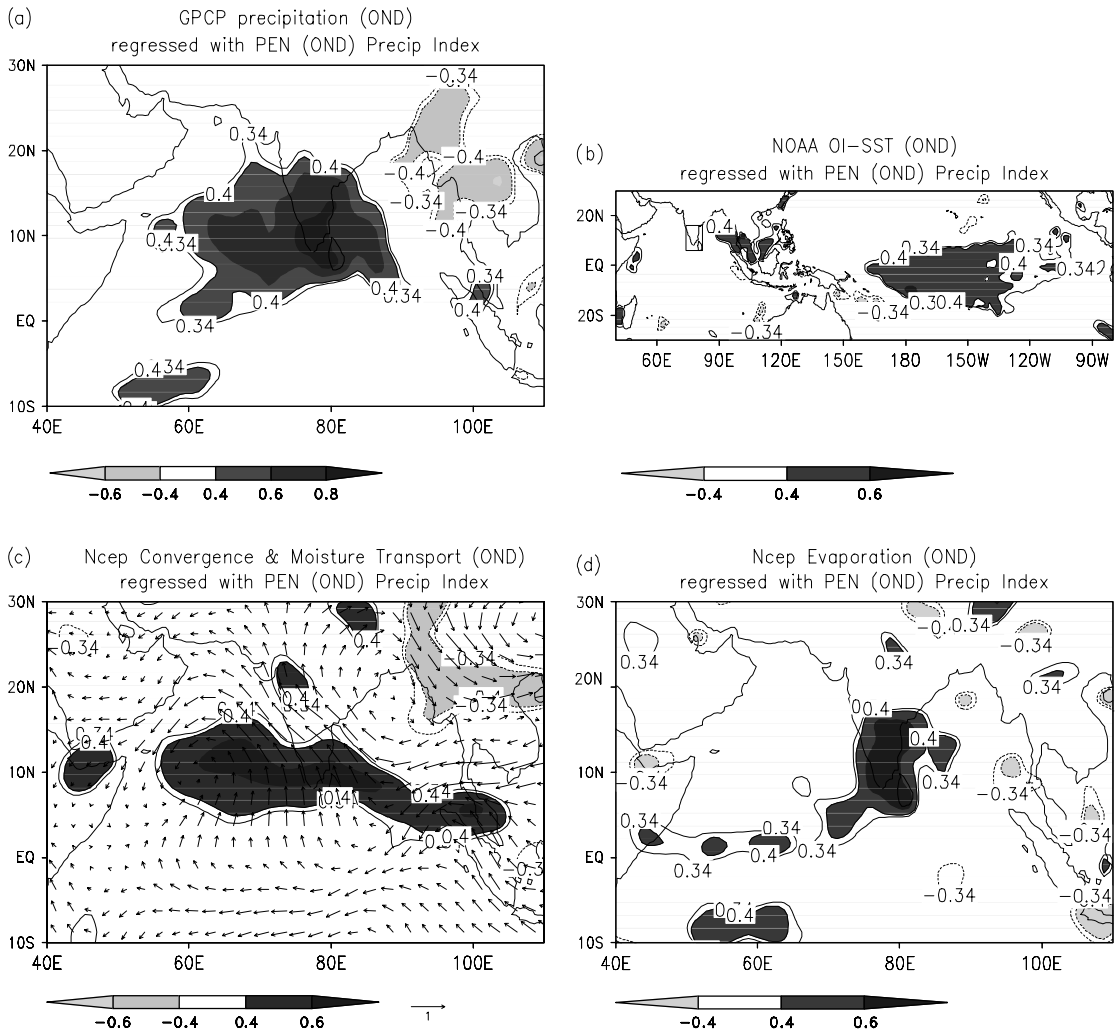

Figure 6. Regression maps based on PEN and SL domain GPCP precipitation. Top panel: (a) GPCP Precipitation, (b) OND SST (domain encompassing PEN & SL is shown by a box). Lower panel: (c) NCEP moisture convergence and moisture flux transport, (d) NCEP evaporation. (95% significant levels are shaded and 90% are just contoured). (Shades indicate regression coefficient; units for precipitation, convergence and evaporation: mm/day, SST:°C, moisture flux: kg m^{-1} s^{-1}).

DOI: 10.1002/joc

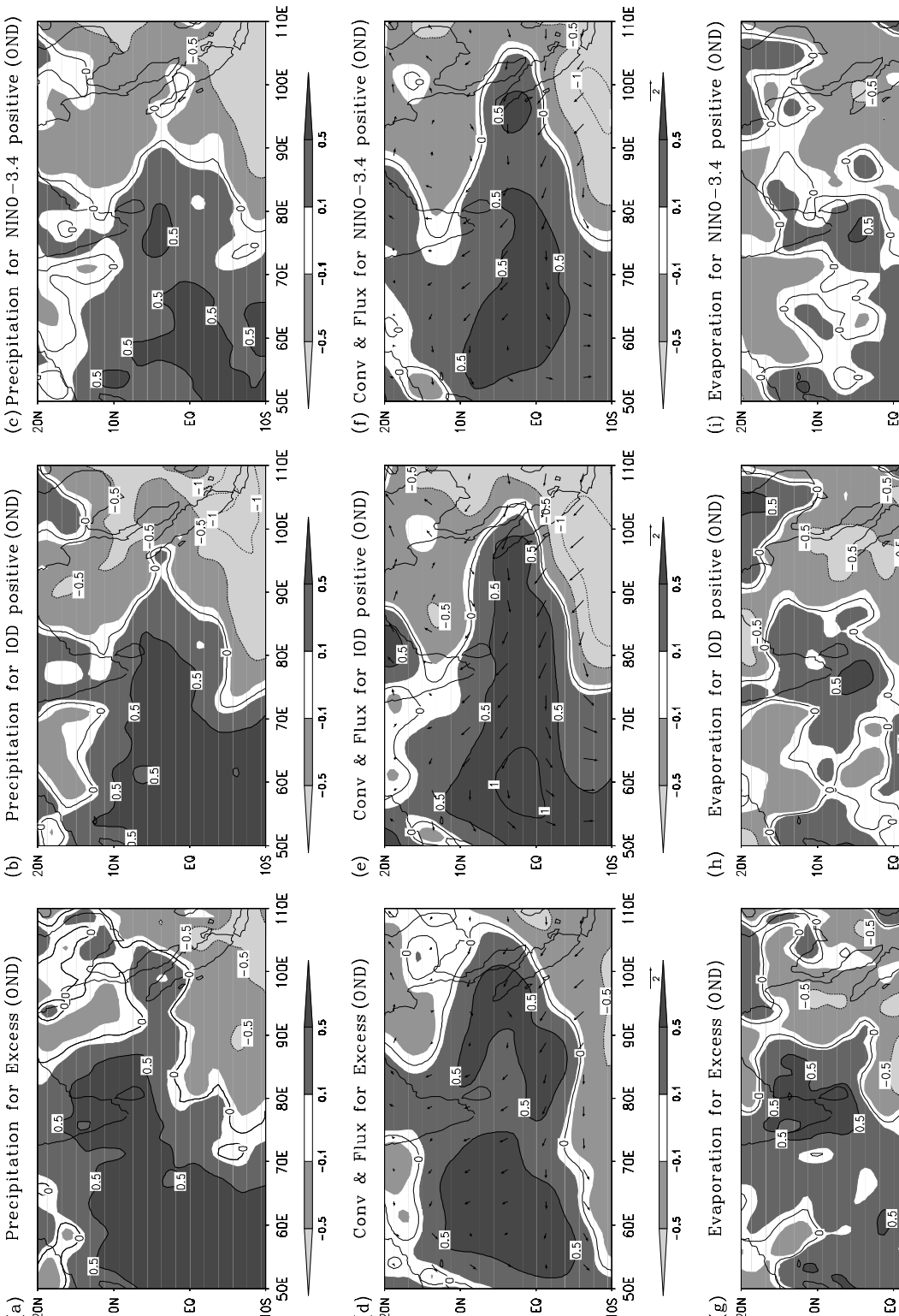

Figure 7. Standardized anomaly maps based on excess and Indian Ocean dipole positive mode phase and NINO-3.4 positive anomaly phase. Top panel: GPCP precipitation for (a) excess year (OND), (b) IOD positive phase, (c) NINO-3.4 positive phase. Middle panel: Moisture convergence and moisture flux transport for (d) excess year, (e) IOD positive phase, (f)NINO-3.4 positive phase. Bottom panel: Evaporation for (g) excess year, (h) positive phase, (i) NINO-3.4 positive phase. (Positive anomalies are darkly shaded and negative anomalies are lightly shaded). (Units for precipitation, convergence and evaporation: mm/day, moisture flux: kg m^{-1} s^{-1}).

DOI: 10.1002/joc

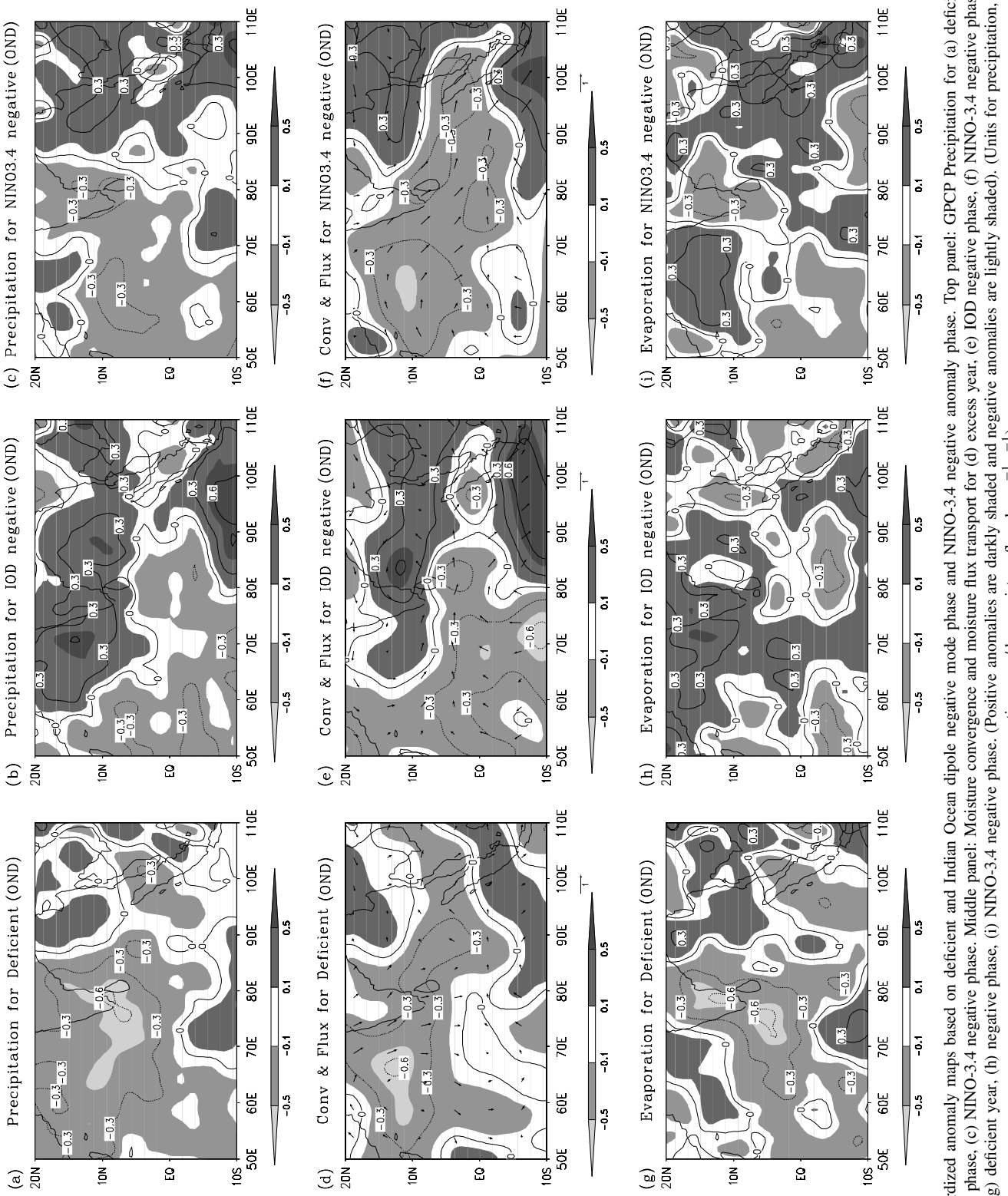

Figure 8. Standardized anomaly maps based on deficient and Indian Ocean dipole negative mode phase and NINO-3.4 negative anomaly phase. Top panel: GPCP Precipitation for (a) deficient year (OND), (b) IOD negative phase, (c) NINO-3.4 negative phase. Middle panel: Moisture convergence and moisture flux transport for (d) excess year, (e) IOD negative phase, (f) NINO-3.4 negative phase. Bottom panel: Evaporation for (g) deficient year, (h) negative phase, (i) NINO-3.4 negative phase. (Positive anomalies are darkly shaded and negative anomalies are lightly shaded). (Units for precipitation, convergence and evaporation: mm/day, moisture flux: kg m^{-1} s^{-1}).

DOI: 10.1002/joc

Table I. Selected cases of excess NEMR, deficient NEMR, IOD positive, negative phases and El Nino, La Nina phases.

Excess NEMR	Deficient NEMR	IOD positive	IOD negative	El Nino	La Nina
1993	1983	1982	1984	1982	1983
1994	1984	1991	1990	1986	1984
1997	1986	1994	1992	1987	1985
2002	1988	1997	1993	1991	1988
2005	1989	2002	1996	1994	1995
–	1990	–	1998	1997	1998
–	1995	–	2005	2002	1999
–	2000	–	–	2004	2000

Data period: 1979–2005

also Nino-3.4 anomaly phase years in order to understand the physical mechanism or dynamics through which P variability over the domain occur.

The excess or deficient years are obtained by applying the criterion that the standardized anomalies exceeds ± 0.5 SD. Similarly the IOD and NINO-3.4 phases are also selected by applying the same criterion.

Five excess years, eight deficient years, five IOD positive phases, seven IOD negative phase, eight El Nino phases and eight La Nina phases were selected from (1982–2005) 24 years dataset for analysis as shown in Table I. The excess and deficient years composite anomaly from the seasonal mean climatology are plotted to understand the difference between different phases and their mechanism.

The dynamics of the NEMR–IOD relationship are examined using the P, C and E by constructing standardized anomaly composite patterns for each phase. The excess precipitation composite anomaly pattern (Figure 7(a)) is generally caused by enhanced convergence and enhanced moisture transport from the southeast Indian Ocean and the south Bay of Bengal towards south peninsular India and Sri Lanka (Figure 7(d)). The evaporation composite anomaly is also positive during excess years (Figure 7(g)). The precipitation anomaly in (Figure 7(a)) is similar to the positive IOD phase composite anomaly pattern (Figure 7(b)) and also similar to the El-Nina composite anomaly pattern (Figure 7(c)). Similarly, the convergence composite anomalies (Figure 7(d)) over the equatorial IO resembles IOD phase (Figure 7(e)) as well as El Nino phase (Figure 7(f)), except a slight higher divergence over BOB region in both IOD and El Nino phases. Evaporation anomaly over the domain is slightly positive during the excess years (Figure 7(g)) compared to IOD positive phase (Figure 7(h)) and El Nino phase (Figure 7(i)). Thus the overall features of excess NEMR seems to be influenced by the combined effect of IOD positive and El Nino phases. So we can say that positive NEMR is approximately equal to the effects of positive IOD phase and El Nino phase.

Standardized composite anomaly for deficient NEMR, IOD negative and La Nina phases are shown in Figure 8. The deficient NEMR precipitation composite anomaly pattern (Figure 8(a)) shows very strong deficient precipitation, associated with strong divergence and enhanced anti-cyclonic moisture transport over the Arabian Sea and South Peninsular India and Sri Lanka and the adjacent oceanic regions (Figure 8(d)). The evaporation composite anomaly is also negative during the deficient years (Figure 8(g)). The precipitation anomaly over the domain during deficient years (Figure 8(a)) is not similar to the negative IOD phase composite precipitation anomaly pattern (Figure 8(b)), but has some similarity to the La Nina composite precipitation anomaly pattern (Figure 8(c)), still the precipitation anomaly during deficient years is quite stronger compared to La Nina composite precipitation anomaly pattern. The IOD negative phase induces precipitation anomaly over the equatorial IO, but has little impact on South Peninsular India and Sri Lanka as we can notice positive precipitation anomaly over South Peninsular India and adjacent region during IOD negative phase (Figure 8(b)). Similarly, the convergence composite anomaly for negative IOD phase (Figure 8(e)) is confined to the equatorial IO, convergence over SEIO and BOB and divergence over equatorial WIO, which does not resemble the deficient composite anomaly phase (Figure 8(d)) as well as La Nina phase (Figure 8(f)). The composite convergence anomaly pattern during the deficient phase (Figure 8(d)) and La Nina anomaly pattern (Figure 8(f)) are quite similar. And also the evaporation composite anomaly for deficient years (Figure 8(g)) is similar to La Nina anomaly years (Figure 8(i)) and does not compare with negative IOD years (Figure 8(h)). Thus the overall features of deficient NEMR seems to be influenced only by La Nina phase. So we can say, negative NEMR is approximately equal to the effects of the La Nina phase.

The asymmetrical influence of IODM on the NEMR is also evident in the composite anomaly maps of SST. Figure 9(a)–(c) shows the SST composite anomaly for NEMR excess years, IOD positive phase and El Nino phase respectively. The patterns more or less agree with one another, except that the IOD phase anomaly composite shows enhanced east–west dipole mode (Figure 9(b)). Both in excess NEMR and El Nino phases, the east–west dipole is subdued (lower magnitude of anomalies on either side). So we can say that the excess NEMR monsoon is favoured by colder SST anomalies over the tropical SEIO and warmer SST anomalies over tropical WIO (a typical IOD positive phase) associated with the El

DOI: 10.1002/joc

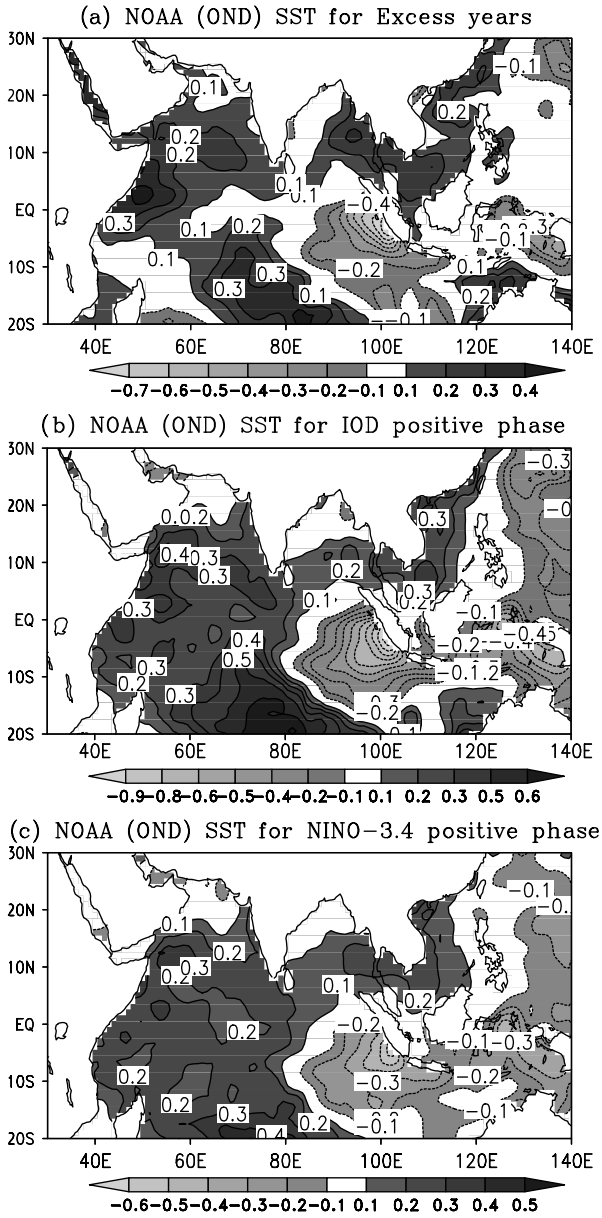

Figure 9. NOAA composite SST anomaly maps based on NEMR excess years, Indian Ocean dipole positive mode phase and NINO-3.4 positive anomaly phase.(a) for excess years (OND), (b) for IOD positive phase, (c) for NINO-3.4 positive phase. (Positive anomalies are darkly shaded and negative anomalies are lightly shaded). (Units for SST anomaly: °C).

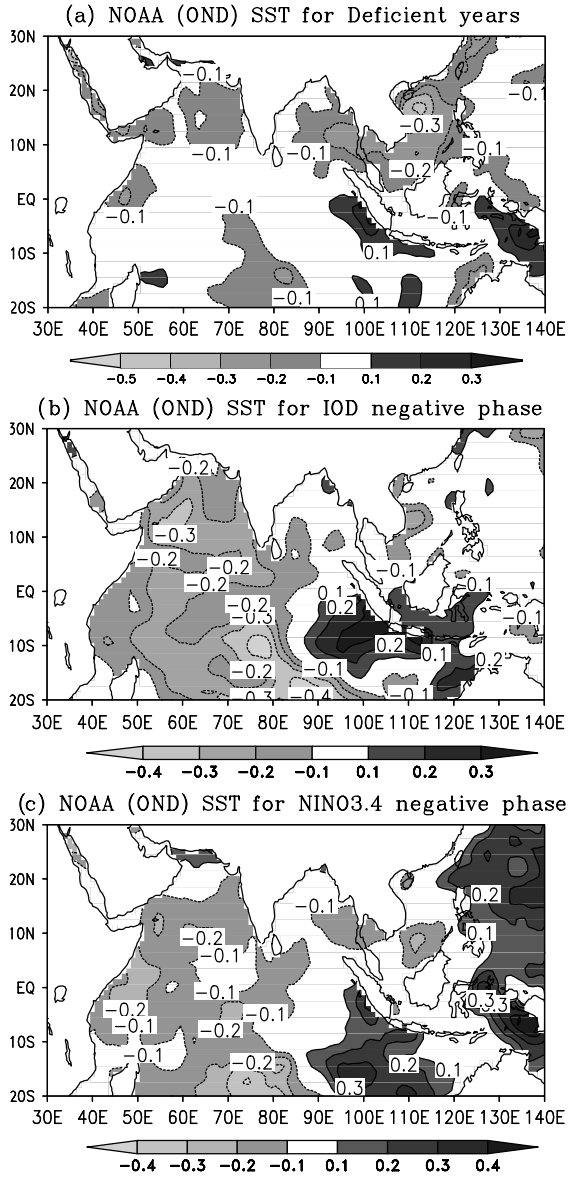

Figure 10. NOAA composite SST anomaly maps based on NEMR deficient years, Indian Ocean dipole negative mode phase and NINO-3.4 negative anomaly phase.(a) deficient years (OND), (b) IOD negative phase, (c) NINO-3.4 negative phase. (Positive anomalies are darkly shaded and negative anomalies are lightly shaded). (Units for SST anomaly: °C).

Nino conditions over tropical Pacific Ocean. Moreover, the SST anomalies over the BOB is also important as this basin is responsible for generating tropical cyclones, which significantly affect the precipitation over NEMR domain during OND (Kumar *et al*., 2007).

In contrast, Figure 10(a)–(c) shows the SST composite anomaly for NEMR deficient years, IOD negative phase and La Nina phase respectively. In the deficient composite years, the SST pattern over the tropical SEIO exhibits a warmer SST anomaly and colder anomaly over the tropical WIO (Figure 10(a)), but we can notice a large pool of negative anomaly over BOB; this pattern is absent in the IOD negative phase (Figure 10(b)). The negative anomaly over the BOB basin is not favourable for the formation of tropical cyclones, which in turn affect the precipitation over the NEMR domain considerably. The SST composite patterns resemble the La Nina phase quite well (Figure 10(c)), though the pool of SST anomaly is confined to the eastern part of the BOB basin. In the IOD negative phase SST composite pattern (Figure 10(b)), only the east–west SST difference is enhanced, but it is quite different from the La Nina and NEMR deficient years composite patterns.

Therefore, the precipitation (P), SST, convergence (C), evaporation (E) and moisture circulation anomalies associated with the positive IOD and excess NEMR are consistent, whereas the precipitation (P), SST,

DOI: 10.1002/joc

convergence (C), evaporation (E) and moisture circulation anomalies associated with the negative IOD and deficient NEMR are inconsistent. This result suggests evidence of the asymmetrical influence of IODM on the NEMR during OND rainfall over South Peninsular India and Sri Lanka. Moreover, El Nino/La Nina has (basically) symmetrical influence, unlike IOD. IOD influence is confined only to positive NEMR.

Apart from the ocean-atmospheric interactions, we notice some land-atmosphere interactions too. Recently, by using ensembles of GCM models Koster *et al*. (2004) showed that soil moisture hot spots exist over some relatively dry monsoon regions. The land-atmospheric interactions over these domains are crucial in understanding the soil moisture impact on precipitation. They have shown that over the transition zones between wet and dry climates, soil moisture anomalies are translated into precipitation anomalies. In dry climates, evaporation rates are sensitive to soil moisture, but are also generally small and small evaporation rates should have a limited ability to affect precipitation. Only in the transition zones between wet and dry climates, the atmosphere is conducive for generation of precipitation where evaporation is suitably high but still sensitive to soil moisture, so we can expect soil moisture to influence precipitation (in particular, where boundary layer moisture can trigger moist convection). The excess evaporation during the entire season OND as observed in Figure 3(b) may support such a hypothesis based on GCM results. We may notice significant and strong regression coefficient of evaporation also over land apart from adjacent oceanic regions in the domain (large-scale residual evaporation regressed with the domain precipitation) (Figure 6(d)). But the validity of such hypothesized processes requires a much more detailed study. Thus, the positive (+NEMR) case is favoured by both evaporation from land surface and enhanced evaporation from positive SST (+SST) over BOB, while during negative (−NEMR), large-scale downward motion due to La Nina inhibits higher evaporation over land and adjacent oceans.

8. Conclusions and discussion

We investigated the interannual variability of atmospheric water balance components over South Peninsular India and Sri Lanka during NEMR (OND) season and summarize our results as follows:

1. Asymmetrical influence of IODM on the NE monsoon rainfall anomaly during OND over South Peninsular India and Sri Lanka.

   The precipitation (P), SST, convergence (C), evaporation (E) and moisture circulation anomalies associated with a positive IOD and NEMR excess years are consistent, whereas the precipitation (P), SST, convergence (C), evaporation (E) and moisture circulation anomalies associated with negative IOD and NEMR deficient years are inconsistent. This result suggests that the influence of IODM on the NEMR is not symmetrical, whereas an asymmetrical influence of IODM on the NEMR is evident.
2. Apart from strong ocean-atmospheric interactions, some land-atmospheric interactions do co-exist over this domain.

The contribution of evaporation (E) is higher for seasonal mean precipitation (P) over the domain; the interannual variability of precipitation (ΔP) is determined not only by evaporation (ΔE), but also by the large-scale convergence (ΔC).

The interannual variability of precipitation over South Peninsular India and Sri Lanka is mainly influenced by both evaporation over land and adjacent oceans and large-scale moisture convergence from the south IO region is evident from the water budget analysis. However, the large-scale circulation anomalies can modulate evaporation over the domain and subsequently modulate precipitation. Mainly, evaporation over the adjacent oceanic regions acts as the source of moisture for precipitation, still evaporation over land is also considerably high. Land surface processes over the domain during NEMR monsoon season may also play a role in modulating precipitation anomalies. However, one has to keep in mind that the grid resolution of the model (reanalysis) is relatively poor and the calculated C and observed P may have errors, but still the relative role of land surface hydrological processes cannot be ruled out and further studies are required to understand the role of land surface processes in modulating the precipitation anomalies over this region during NEMR (OND) season. The major findings of this study are also briefly summarized in Table II.

Therefore, we discuss that the land, the atmosphere and the ocean interactively modulate the NEMR over South Peninsular India and Sri Lanka during OND. So far, the existence of the hot spots of land-atmosphere interactions of significant coupling strength in relatively dry monsoon regions during summer monsoon (JJAS) season are known from an ensemble of GCM studies (e.g. Koster *et al*., 2004). From our study, we have found that the land surface processes may also contribute to precipitation anomalies over South Peninsular India and Sri Lanka during (OND) NE monsoon season.

Table II. Summary of major findings from the study.

NEMR variability	IOD conditions		Nino 3.4 conditions	
	Positive	Negative	El Nino	La Nina
NEMR positive	Yes	–	Yes	–
i.e. NEMR positive ∼ IOD positive + El Nino				
NEMR negative	–	No	–	Yes
i.e. NEMR negative ∼ La Nina (only)				

DOI: 10.1002/joc

Acknowledgement

We would like to thank Drs Fujinami, Hori, Takahashi, Abe, Ichikawa and Mr Kanamori for their helpful comments during this research work. We also would like to thank two anonymous Referees for their encouraging comments. VP was supported by Monbukagakusho scholarship from the ministry of Education, Culture, Sports, Science and Technology. We also acknowledge many centres for providing datasets. NCEP/NCAR Reanalysis and NOAA_OI_SST_V2 data provided by the NOAA/OAR/ESRL PSD, Boulder, Colorado, USA, from their web site at (http://www.cdc.noaa.gov/) and VASClimO dataset from (http://www.deutscherwetterdienst.de/). VASClimO is an activity of the German Weather Service. The diagrams used for this study have been prepared using the free software packages like GrADS and XMGRACE and computational work done on the Fedora Core 2 operating system environment.

References

Adler RF, Huffman GJ, Chang A, Ferraro R, Xie P, Janowiak J, Rudolf B, Schneider U, Curtis S, Bolvin D, Gruber A, Susskind J, Arkin P, Nelkin E. 2003. The Version 2 Global Precipitation Climatology Project (GPCP) Monthly Precipitation Analysis (1979–Present). *Journal of Hydrometeorology* **4**: 1147–1167.

Ailikun B, Yasunari T. 2001. ENSO and Asian summer monsoon: persistence and transitivity in the seasonal march. *Journal of the Meteorological Society of Japan* **79**: 145–159.

Beck C, Grieser J, Rudolf B. 2005. A new monthly precipitation climatology for the global land areas for the period 1951 to 2000. *Climate Status Report* **2004**: 181–190.

Chang CP, Harr P, Ju J. 2001. Possible roles of Atlantic circulations on the weakening Indian monsoon rainfall-ENSO relationship. *Journal of Climate* **14**: 2376–2380.

Dhar ON, Rakhecha PR. 1983. Forecasting northeast monsoon rainfall over Tamil Nadu, India. *Monthly Weather Review* **111**: 109–112.

Hastenrath S, Nicklis A, Greischar L. 1993. Atmospheric hydrospheric mechanisms of climate anomalies in the western equatorial Indian Ocean. *Journal of Geophysical Research* **98**: 20,219–20,235.

Kalnay E, Kanamitsu M, Kistler R, Collins W, Deaven D, Gandin L, Iredell M, Saha S, White G, Woollen J, Zhu Y, Chelliah M, Ebisuzaki W, Higgins W, Janowiak J, Mo KC, Ropelewski C, Wang J, Leetmaa A, Reynolds R, Jenne Roy, Joseph Dennis. 1996. The NCEP/NCAR 40-Year Reanalysis Project. *Bulletin of the American Meteorological Society* **77**(3): 437–471.

Kawamura R, Uemura K, Suppiah R. 2005. On the recent change of the Indian summer monsoon-ENSO relationship. *SOLA* **1**: 201–204.

Koster RD, GLACE Team. 2004. Regions of strong coupling between soil moisture and precipitation. *Science* **305**: 1138–1140.

Kripalani RH, Kumar P. 2004. Northeast monsoon rainfall variability over south peninsular India vis-a-vis the Indian Ocean dipole mode. *International Journal of Climatology* **24**: 1267–1282.

Krishna Kumar K, Rajagopalan B, Cane MA. 1999. On the weakening relationship between the Indian monsoon and ENSO. *Science* **284**: 2156–2159.

Oki T, Musiake K, Matsuyama H, Masuda K. 1995. Global atmospheric water balance and runoff from large river basins. *Hydrological Processes* **9**: 655–678.

Kumar P, Rupa Kumar K, Rajeevan M, Sahai AK. 2007. On the recent strengthening of the relationship between ENSO and northeast monsoon rainfall over South Asia. *Climate Dynamics* **28**: 649–660.

Peixoto JP, Oort AH. 1992. *Physics of Climate*. American Institute of Physics, Springer Verlag; 520, ISBN: 0883187124.

Rasmusson EM, Carpenter TH. 1983. The relationship between eastern equatorial Pacific sea surface temperatures and rainfall over India and Srilanka, *Monthly Weather Review* **111**: 517–528.

Reynolds RW, Rayner NA, Smith TM, Stokes DC, Wang W. 2002. An improved in situ and satellite SST analysis for climate. *Journal of Climate* **15**: 1609–1625.

Saji NH, Yamagata T. 2003. Possible impacts of Indian Ocean dipole mode events on global climate. *Climate Research* **25**: 151–169.

Saji NH, Goswami BN, Vinayachandran PN, Yamagata T. 1999. A dipole mode in the tropical Indian Ocean. *Nature* **401**: 360–363.

Singh N, Sontakke NA. 1999. On the variability and prediction of post-monsoon season rainfall over India. *International Journal of Climatology* **19**: 309–339.

Suppiah R. 1989. Relationship between the southern oscillation and the rainfall of Sri Lanka. *International Journal of Climatology* **9**: 601–618.

Suppiah R. 1996. Spatial and temporal variations in the relationship between southern oscillation phenomenon and the rainfall of Sri Lanka. *International Journal of Climatology* **16**: 1391–1407.

Suppiah R. 1997. Extremes of southern oscillation phenomenon and the rainfall of Sri Lanka. *International Journal of Climatology* **17**: 87–101.

Trenberth KE. 1999. Atmospheric moisture recycling: role of advection and local evaporation. *Journal of Climate* **12**: 1368–1381.

Trenberth KE, Guillemot CJ. 1998. Evaluation of the atmospheric moisture and hydrological cycle in the NCEP/NCAR reanalyses. *Climate Dynamics* **14**: 213–231.

Webster PJ, Moore AM, Loschnigg JP, Leben RR. 1999. Coupled ocean-atmosphere dynamics in the Indian Ocean during 1997–98. *Nature* **401**: 356–360.

Yasunari T. 1990. Impact of Indian monsoon on the coupled atmosphere/ocean systems in the tropical pacific. *Meteorology and Atmospheric Physics* **44**: 29–41.

Zubair L, Rao SA, Yamagata T. 2003. Modulation of Sri Lankan Maha rainfall by the Indian Ocean dipole. *Geophysical Research Letters* **30**(2): 35–1–35–4.

DOI: 10.1002/joc